Summer Scholar Report

The effect of acid in hydrothermal conversion of titanium nitride into titanium dioxide for use in photocatalysis

By Cameron McInnes, Department of Chemistry and Materials Science Program, University of New Hampshire, Durham, New Hampshire 03824, United States

Abstract

In titanium dioxide (TiO_2) photocatalysis, it is well established that the morphology of TiO_2 particles has a significant effect on the photocatalytic properties. In this study, different acids were used in the hydrothermal synthesis of TiO_2 from titanium nitride to observe the effect of acid choice. While there are examples in the literature using various acids, there is little emphasis placed on controlling morphologies using the acid-assisted hydrothermal synthesis. In some cases other synthetic parameters were varied, including acid concentration, hydrothermal heating time, and calcination temperature. We show results obtained from scanning electron microscopy, a photocatalysis test, X-ray powder diffraction analysis, and, when applicable, the comparison with commercially available P25 TiO_2. Our findings contribute to the future development of TiO_2-based photo- catalysts for efficient solar energy conversion.

Introduction

Solar energy conversion by photocatalysis is a promising technology that can displace combustive methods of energy generation[1] and help to remove environmental pollutants.[2] The conversion and storage of solar energy to chemical energy is seen in solar fuel generation via CO_2 reduction. Photocatalytic oxidation has been utilized to degrade organic molecules into harmless products. Titanium dioxide (TiO_2) is especially promising due to its stability, non-toxicity, noncorrosive properties, its abundance, and it's low cost.[2,3] In addition, the material's electronic properties, such as appropriate band gap, allow for CO_2 reduction and water splitting.[4] The products of these two processes, CO and H_2, are very valuable for the facility with which they can be transformed into liquid hydrocarbon fuels using the Fischer-Tropsch reaction.[2,5-7] A closed system, powered by sunlight, could generate sustainable energy with virtually no pollutants.

The challenges of TiO_2 photocatalysis include charge recombination and minimal visible light absorption.[4,8] Charge recombination in a photocatalytic semiconductor is the process of a photoexcited electron in the conduction band (CB) returning to the valence band (VB, Figure 1). Photoexcitation is a process in which a photon from the sun transfers its energy into an electron of the TiO2 particle. The excited electron, which is now in the CB, leaves a positively charged hole, denoted h+, in its place. Either of these species may diffuse to the surface of the particle and become available for chemical reactions, unless the electron and hole recombine due to attractive forces. Upon recombination, the light energy is dissipated as thermal energy and no chemical reaction occurs.

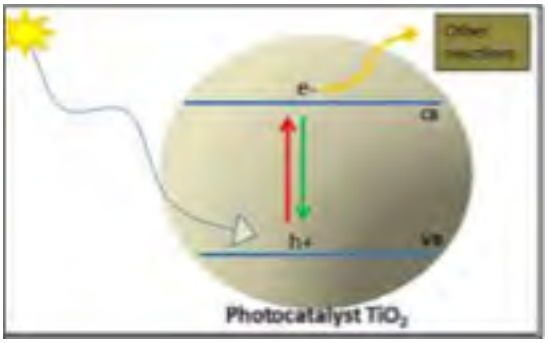

Figure 1.Electron (e-) is excited to CB (red arrow), generating a hole (h+), where it can either be utilized in another reaction (yellow arrow), or it recombines (green arrow), returning to the valence band.

Methods of inhibiting recombination include adding electron or hole scavengers and optimizing the surface characteristics of the particle.[4] These methods can improve charge separation. Effective charge separation can also be achieved through morphology modification. Optimized nanoparticles, as opposed to micron-sized particles, exhibit less charge recombination.[4] Nanorods have been synthesized to have higher surface-to-volume ratios than that of nanospheres[9] and allow for creative organizational structures.[10-11]

The wide band gap, or high 'activation energy', of TiO_2 materials limits the photoresponse of these materials to the higher energy ultraviolet region. The sun emits significantly more photons in the lower energy visible light region, which, if utilized, would greatly increase overall solar efficiency. Nitrogen-doping of TiO_2 materials has arisen as a promising solution to poor visible light absorption.[13-15] This process simply replaces a small fraction of the oxygen molecules in TiO_2 with nitrogen. The result is a modification of the electronic properties of the TiO_2 material. The energy required to excite an electron from the valence band to the conduction band, or band gap, is reduced, potentially allowing for visible light photocatalysis.

The solution to both of these problems can be achieved through optimizing TiO_2 materials in terms of color, size, shape, phase, and presence of dopant. The synthesis of TiO_2 from a titanium nitride precursor has been previously achieved via different methods, including open air annealing,[16,17] hydrothermal treatment with H_2O_2,[18] and hydrothermal treatment with acid.[19,20] In this study, we attempt to understand how much synthetic control can be had over surface morphology through the variation of simple synthetic parameters. The type of acid, acid concentration, hydrothermal treatment time, and calcination temperature were the varied parameters in our study.

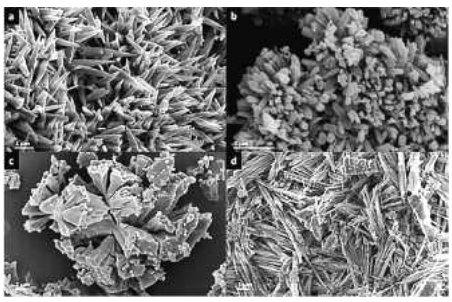

Figure 2. Four acids at a final concentration of 2M were explored in the synthesis of TiO_2 (a. hydrochloric acid, b. nitric acid, c. sulfuric acid, d. phosphoric acid).

Experimental Procedure

In a typical synthesis, 0.31 g of titanium nitride (Alfa Aesar, 99.7%) was added to varying quantities of DI water under magnetic stirring. Acid was then added dropwise over 30 minutes to attain a final volume of 50mL. The mixture was then placed in a Teflon-lined autoclave and heated over a 2-hour period to 180ÅãC and held for various times. After cooling to room temperature, the contents were placed into two 25mL centrifuge tubes and centrifuged at 10000 rpm for 5 minutes. The supernatant was discarded, the tubes were refilled with DI water, sonicated, and resuspended before being centrifuged again. This washing cycle was repeated 4-5 times, until the discarded supernatant pH was above 5. The remaining contents were then transferred to a ceramic bowl to dry for at least 12 hours in a fume hood. The product was ground, sonicated, and calcined. After cooling, the sample was ground and sonicated.

SEM images were collected on an Amray 3300FE scanning electron microscope. X-ray diffraction patterns of TiO_2 powder materials were collected on a Shimadzu XRD-6100 diffractometer. In dye degradation experiments, 45 mg of powder sample were placed in 50 mL of 0.125 mM methylene blue solution. The mixture was stirred for 15 minutes in the dark to allow dye adsorption equilibrium to be established. The mixture was then irradiated with visible light at an intensity of 100 mW/cm^2 from a Fiber-Lite High Intensity Illuminator (Series 180, Dolan-Jenner Industries Inc.) Irradiance was measured with a Newport Hand Held Optical Meter (model 1918 C, +/- 02 mW/cm^2). The light was equipped with a water filter to reduce radiative heating of the reaction vessel from infrared light. Every 15 minutes a 1 mL aliquot was collected and centrifuged at 12,500 rpm for 3 minutes in an Eppendorf (Centrifuge 5425) centrifuge. The absorbance of the supernatant was then measured with UV-Vis spectroscopy at 664 nm.

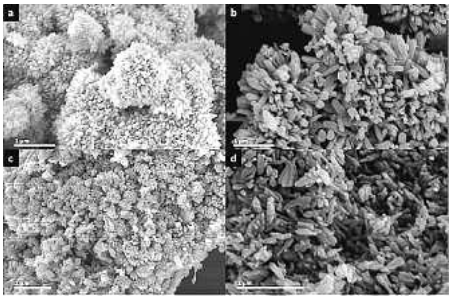

Figure 3. Four acid concentrations were explored in the synthesis using nitric acid (a. 1M, b. 2M, c. 3M, d. 4M).

Results and Discussion

The naming convention of samples is as follows. The first letters correspond to the acid used in synthesis; NA is nitric acid, PA is phosphoric acid, HCl is hydrochloric acid, The next number preceding an 'M' is the acid concentration during the hydrothermal treatment ; 1M, 2M, etc. The next number is the duration of the hydrothermal treatment time; 12 hr, 56 hr, etc. Finally, the calcination temperature is shown; 500^{o}C, 650^{o}C, etc. Samples underwent hydrothermal treatment for 12 hours and were calcined at 500^{o}C unless specified.

Hydrochloric acid was then used in 4M and 8M concentrations, as well as a phosphoric acid in a 4M concentration, showing a steep decrease in nanorod abundance (images not shown).

The morphology of nitric acid samples was not greatly changed in the syntheses, as evidenced in Figure 3. For this acid, in particular, another notable trend was the color of the material. As molarity of nitric acid increased from 1M to 4M, the powder color changed from dark yellow to very light yellow. This observation is observable in the UV-Vis Diffuse Reflectance and XRD analysis below.]

Figure 4. Three calcination temperatures were explored in the synthesis using phosphoric acid in a 2M concentration (a. 500 °C: 5 hours, b. 650 °C: 12 hours, c. 800 °C: 5 hours).

It is observable in Figure 4 that the overall morphology of the phosphoric acid synthesized samples are not significantly changed between 500°C and 650°C calcinations.

Figure 5. Three hydrothermal treatment times were explored in the synthesis involving phosphoric acid in a 2M concentration (a. 12 hours, b. 56 hours, c. 168 hours). The 12 and 56 hour samples were calcined at 650°C, and the 168 hour sample at 800°C.

However, at 800°C, major effects are observable. A slight lightening of the brown color was observed with each increase in calcination temperature.

Figure 5 shows a decrease in particle size and a decrease in amount of amorphous chunks, which are likely unreacted TiN. The 800°C calcination of this sample seemed to combine the rods into amorphous structures, but did not show signs of unreacted TiN.

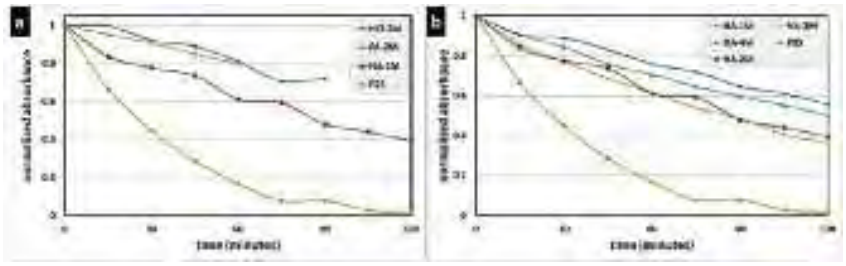

Figure 6. Normalized absorbance of methylene blue at 664 nm as a function of reaction time during visible-light photocatalytic degradation (a. survey of varying acids at 2M concentrations, b. survey of varying acid concentration of nitric acid during synthesis).

The activities of the various acid samples are less than the activity of commercially available P25. As Figure 6a shows, the nitric acid sample is the best performing out of the group of 2M concentrations. The sulfuric acid sample was not tested because of its undesirable color of dark brown, and its amorphous shape. Nitric acid samples in Figure 6b showed little improvement after an attempt to optimize the particle by varying acid concentration during synthesis, with the 3M concentration performing slightly better.

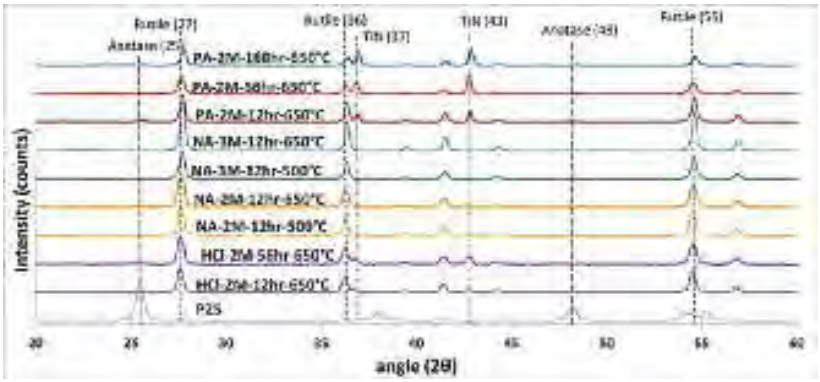

Figure 7. XRD analysis of samples confirm a mostly rutile composition with some peaks matching those of the precursor titanium nitride (TiN).
Nine representative samples are seen in this figure, showing the closeness in composition of all samples. P25 is also shown for reference.

We can conclude from Figure 7 that the hydrothermal synthesis of TiN in an acid-water mixture produces rutile phase TiO_2 with varying amounts of TiN. The intensity of peaks at 2 = 37°, 43° in the XRD scan, combined with physical observation, indicates a correlation with TiN presence and the darkness of the powder. Due to the reduction of the TiN peaks between samples calcined at 500°C and 650°C (most evident in the NA-2M-12hr samples, orange), we can conclude that the calcination at elevated temperature reacted TiN into TiO_2. Also observable is a decrease of the 37° peak of TiN between the 2 and 3 M nitric acid samples.

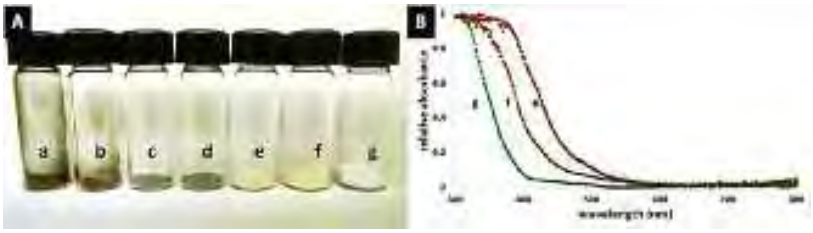

Figure 8. A: A digital image showing the different color powders synthesized with varying acids (a. pure TiN, b. HCl-2M, c. PA-2M, d. NA-1M, e. NA-2M, f. NA-4M, g. commercial P25-TiO_2). B: UV-visible diffuse reflectance spectra of selected samples (g. P25-TiO_2, f. NA-4M, e. NA- 2M).

This, along with the visible color difference, indicates that as molarity of nitric acid is increased, the presence of TiN decreases. The wide array of powder color observed lies between the colors of the original reagent, TiN, and the fully oxidized form, TiO_2. Along with the XRD analysis, this depicts a model where powder color is dependent on TiN concentration, which was controlled by acid concentration. The UV-Vis shows that the presence of nitrogen in TiO_2 particles shifts the threshold of light absorbance, or band gap, which agrees with literature.[21,22]

Conclusion

Samples were synthesized through hydrothermal treatment of titanium nitride in an acid-water solution. By varying simple synthetic parameters, effects on morphology and photocatalytic activity were observed. In our experiments, hydrothermal syntheses using nitric acid concentrations between 1M and 4M, 500ÅãC calcination temperatures, and 12-hour hydrothermal reaction times resulted in yellow powders consisting of short flower-shaped nanorods which demonstrated favorable catalytic qualities such as visible-light methylene blue degradation. As acid concentration was increased, the TiN concentration was decreased, as evidenced by XRD and UV-Visible diffuse reflectance spectra. Syntheses using 2M concentrations of hydrochloric acid,

500°C calcination temperatures, and 12-hour reaction times produced a grey powder consisting of many long flower-shaped nanorods which were inactive in visible-light methylene blue degradation. Phosphoric acid used in 2M concentrations, with widely varying hydrothermal heating times, and 500-650°C calcination temperatures produced a grey powder consisting of many nano- to micro-scale rods, which may make good foundations for further nanoparticle deposition.

Techniques of altering the band gap and hence the color of powders, most notably hydrochloric and phosphoric acid samples, will be further explored in the future.

Acknowledgements
I thank Ram Subedi, Dr. Mark Townley, Nancy Cherim, and Dr. James Krzanowski for their assistance. I thank Dr. Gonghu Li's Research Group for assistance in and out of the lab and their helpful discussions. This research is supported by a James Flack Norris/Theodore Williams Richards Summer Research Scholarship.

References

1. N. Lewis, D. Nocera. Powering the planet: Chemical challenges in solar energy utilization. PNAS. **2006**, 103, 15729.
2. C. Liao, C. Huang, J.C.S. Wu. Hydrogen Production from Semiconductor-based Photocatalysis via Water Splitting. Catalysts **2012**; 2, 490-516.
3. Sigma-Aldrich. (**2014**, July 10). Titanium(IV) oxide [Material Data Safety Sheet]. Retrieved from: http://www.sigmaaldrich.com/catalog/product/sial/14021?lang=en&region=US
4. He He, Chao Liu, Kevin D. Dubois, Tong Jin, Michael E. Louis, Gonghu Li. Enhanced Charge Separation in Nanostructured TiO_2 Materials for Photocatalytic and Photovoltaic Applications. Ind. Eng. Chem. Res. **2012**, 51, 11841.
5. T.W. Woolerton et al. Efficient and Clean Photoreduction of CO_2 to CO by Enzyme-Modified TiO_2 Nanoparticles Using Visible Light. J. Am. Chem. Soc. **2010**, 132(7), 2132–2133
6. T. Jin, C. Liu, G. Li. Photocatalytic CO_2 reduction using a molecular cobalt complex deposited on TiO_2 nanoparticles. Chem. Commun. **2014**, 50, 6221-6224
7. A.Y. Khodakov, W. Chu, P. Fongarland. Advances in the Development of Novel Cobalt Fischer Tropsch Catalysts for Synthesis of Long-Chain Hydrocarbons and Clean Fuels. Chem. Rev. **2007**, 107, 1692–1744.
8. A.L. Linsebigler, G. Lu, J.T. Yates Jr. Photocatalysis on TiO_2 Surfaces: Principles, Mechanisms, and Selected Results. Chem. Rev. **1995**, 95, 735-758
9. H.Sangjin et al. Low-Temperature Synthesis of Highly Crystalline TiO_2 Nanocrystals and their Application to Photocatalysis. Comm. **2005**, 1, 812-816
10. L.Miaoqiang et al. Densely aligned rutile TiO_2 nanorod arrays with high surface area for efficient dye-sensitized solar cells. Nanoscale, **2012**, 4, 5872.
11. X.He, C.Hu, B.Feng, B.Wan, Y.Tian. Vertically aligned TiO_2 Nanorod Arrays as a Steady Light Sensor. J. Electrochem. Soc., **2010**, *157(11)*, 381-385
12. C. Burda et al. Enhanced Nitrogen Doping in TiO_2 Nanoparticles. Nano Letters **2003**, 3, 1049-1051
13. H. Jie et al. Nitrogen-doped TiO_2 nanopowders prepared by chemical vapor synthesis: bad structure and photocatalytic activity under visible light. Research on Chemical Intermediates **2012**, 38(6), 1171-1180
14. M. Sathish, B. Viswanathan,R. P. Viswanath, C.S. Gopinath. Synthesis, Characterization, Electronic Structure, and Photocatalytic Activity of Nitrogen-Doped TiO_2 Nanocatalyst. *Chem. Mater.* **2005**, *17*, 6349-6353
15. Y. Cong, J Zhang, F. Chen, M. Anp. Synthesis and Characterization of Nitrogen-Doped TiO_2 Nanophotocatalyst with High Visible Light Activity. *J. Phys. Chem. C* **2007**, *111*, 6976-6982

16. Z. Xie et al. Tuning the optical bandgap of TiO_2-TiN composite films as photocatalyst in the visible light. AIP Advances **2013**, 3, 62129
17. Z. Wu, F. Dong, W. Zhao, S. Guo. Visible light induced electron transfer process over nitrogen doped TiO_2 nanocrystals prepared by oxidation of titanium nitride. J. Haz. Mat. **2008**, 157, 57-63
18. D.L. Shieh et al. N-doped, porous TiO_2 with rutile phase and visible light sensitive photocatalyic activity. Chem. Commun. **2012**, *48*, 2528-2530
19. S Wang et al. Facile synthesis of nitrogen self-doped rutile TiO_2 nanorods. CrystEngComm **2012**, *14*, 7672-7679
20. X. Zhou, F. Peng, H. Wang, H. Yu, J. Yang. Preparation of nitrogen doped TiO_2 photocatalyst by oxidation of titanium nitride with H_2O_2. Mat. Research Bulletin **2011**, *46*, 840-844
21. H. Irie, Y. Watanabe, K. Hashimoto. Nitrogen-Concentration Dependence on Photocatalytic Activity of $TiO_{2-x}N_x$ Powders. J. Phys. Chem. *B* **2003**, *107*, 5483- 5486
22. J. Wang, B. Mao, J.L. Gole, C. Burda. Visible-light-driven reversible and switchable hydrophobic to hydrophilic nitrogen-doped titania surfaces: correlation with photocatalysis. Nanoscale **2010**, *2*, 2257-2261